MAREK BIJAK-ŻOCHOWSKI *), *PIOTR MAREK***), *MAREK TRACZ***)*

ON RESIDUAL STRESSES DISTRIBUTIONS DUE TO ELASTO-PLASTIC ROLLING CONTACT

The way of creation and final distribution of residual stress due to the process of rolling contact is of a great interest from cognitive, as well as practical points or view. While residual stress can be created by controlled production process to improve strength properties (e.g. technological cold rolling of pins, threads etc.), they can be introduced also unintentionally in the course of the regular work of the object. Residual stresses in rails are created in this last way; they strongly influence cracking tendencies and the expected life of rails.

Distributions of residual stress due to elasto-plastic rolling contact depend on several factors: magnitude of maximum loading pressure, number of passages during the rolling process, character of the motion (free rolling, rolling with tangential forces due to the brakings and accelerations) etc. However, investigations conducted by different authors have not delivered here any unique solution even for the free rolling contact. Particularly it is not clear what is the distribution of residual stress in the subsurface area, whether and when they can be positive (tensile) at the rolled surface etc.

The aim of this work is the determination of the influence of some of above-mentioned factors on the residual stress distribution.

The analysis has been conducted by the FEM method using the SEGLA program developed by authors, as well as the professional ANSYS program. The numerical results have been broadly verified by the experimental investigations. Experiments

---

*)   *Institute of Aeronautics and Applied Mechanics, Warsaw University of Technology; Nowowiejska 24, 00-665 Warsaw, Poland; E-mail: marta@meil.pw.edu.pl*

**)   *Institute of Aeronautics and Applied Mechanics, Warsaw University of Technology; Nowowiejska 24, 00-665 Warsaw, Poland; E-mail: pmarek@meil.pw.edu.pl*

***) *Institute of Aeronautics and Applied Mechanics, Warsaw University of Technology; Nowowiejska 24, 00-665 Warsaw, Poland; E-mail: mtracz@meil.pw.edu.pl*

have been applied also as a main tool in such cases, where using the numerical methods is still very expensive (if even possible), e.g. for the great number (several thousands) of passages.

1. Introduction

The way of creation and final distribution of residual stress due to the process of rolling contact is of great interest from cognitive as well, as practical points of view. While residual stress can be created by controlled production process to improve strength properties (e.g. technological cold rolling of pins, threads etc.), they can be introduced also unintentionally in the course of the regular work of the object. Residual stresses in rails are created in this last way; they strongly influence cracking tendencies and expected life of rails.

Distributions of residual stress due to elasto-plastic rolling contact depend on several factors. The most important are the magnitude of maximum loading pressure determined in relation to the yield point of the material, as well as the number of passages during the rolling process. Also, the character of the motion (rolling) plays here a great role. For example, a very complex motion of the wheel on the rail consists of the elasto-plastic rolling, elasto-plastic sliding in the longitudinal direction (due to the brakings an accelerations of the train and due to the changeable wheel radius along its width), elasto-plastic sliding in the transversal direction of the rail, etc.

However, investigations conducted by different authors have not delivered here any unique solution even for the free rolling contact. It is not clear what is the distribution of residual stress in the subsurface area, whether and when they can be positive (tensile) at the rolled surface, how the above-mentioned different factors (loading, number of passages, type of motion) change this distribution. On the other hand, it is general conviction among engineers that elasto-plastic rolling process leads to compressive residual stress at the surface of the object. The surface layer is of great importance as an area of cracks development.

The results of numerical calculations for the free-rolling contact, modeled by the travel of the semi-elliptic Hertz pressure distribution on an elasto-plastic half space (Fig. 1) have been presented in Ref. [1]. The absolute values of residual stress components (longitudinal σ_x^r and lateral σ_z^r) drop rapidly approaching the surface; it is not clear, however, whether they are equal to zero or positive (tensile) at the surface (Fig. 2). Practically, they do not depend on the pressure factor p_0/k, which only changes slightly the depth and the shape of the negative residual stress area. The residual stresses are

distinctly smaller than those determined in Kulkarni et al. work (Ref. [2]), which is cited by the authors for comparison.
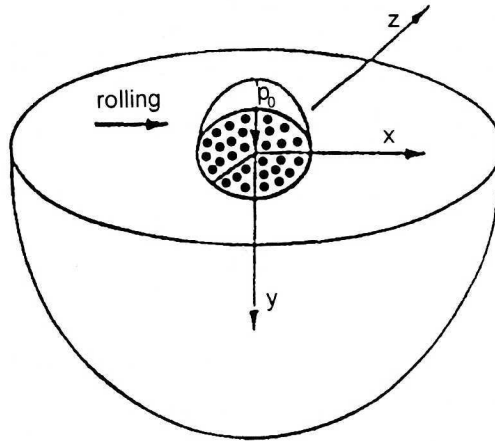

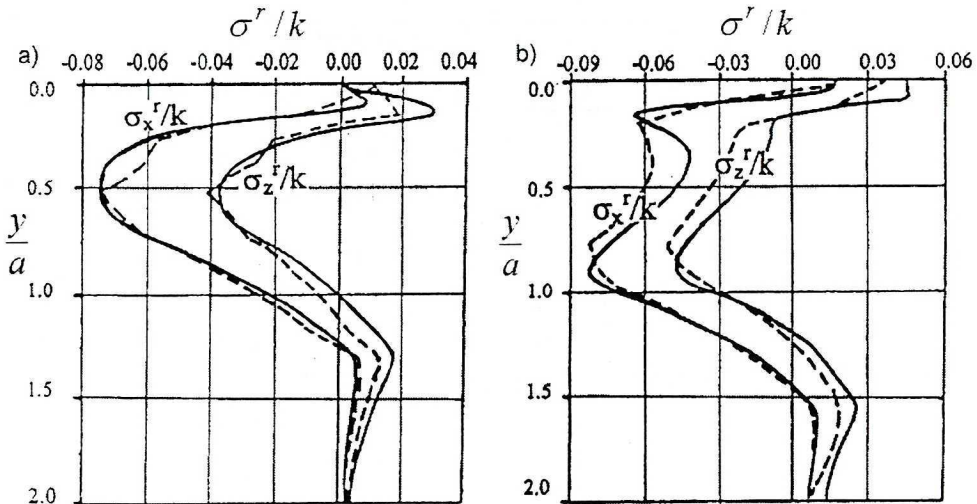Fig. 1. Travel of the semi-elliptic Hertz pressure distribution on an elasto-plastic half-space

Fig. 2. Comparison of residual lateral and longitudinal stress for three-dimensional free rolling according to Ref. [1]: a) $p_0/k = 4,68$; b) $p_0/k = 6.0$. Solid line – authors analysis; dash line – Kulkarni et al. analysis

The numerical analysis of a free rolling contact described in Refs [3] and [4] provides the longitudinal residual stresses distributions (Figures 3 and 4). The results also are not quite clear: the values of residual stresses either are equal to zero in the subsurface layer (Fig. 3), or are slightly positive (tensile) – Fig. 4. In the last case (Fig. 4), the experimental curve, running between two others that describe the results of different numerical approaches, does not indicate residual stress distribution in the discussed area.
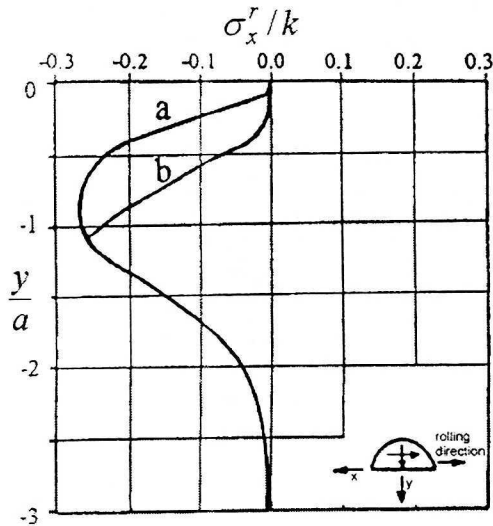
Fig. 3. Two-dimensional free rolling: longitudinal residual stress component distribution, $p_0/k = 5.0$, for homogenous (a) and case – hardened (b) materials (according to Ref. [3])
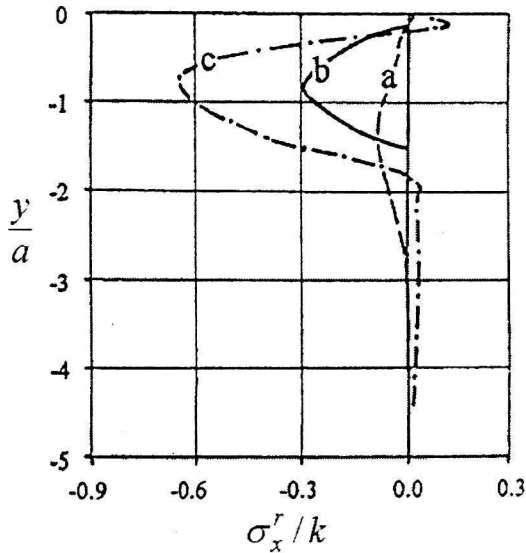

Fig. 4. Two-dimensional free rolling of bearing steel: longitudinal residual stress component distribution: $p_0/k = 6.0$ ($k = 660$ MPa); a) numerical analysis for linear kinematic strain – hardening, b) results of experiments; c) numerical analysis for non-linear kinematic strain hardening (according to Ref. [4])

New plasticity models for elasto-plastic rolling contact applications as well as fatigue crack initiations models are mainly presented in the present works e.g. [5], [6], [7], [8], [9], [10]. However, the problem of distributions of residual stresses in the close vicinity of the running surface has returned into considerations in most recent Refs. [11] and [12]. Number of passages of

a roller and different partial slip conditions strongly influences the results (Fig. 5). After about 40 rolling passes, the values of residual stresses stabilize. Their distribution in the thin subsurface layer depends strongly on the partial slip conditions: the stress on the surface can reach significant positive as well as negative values. The influence of the loading pressure, however, has not been taken into account.
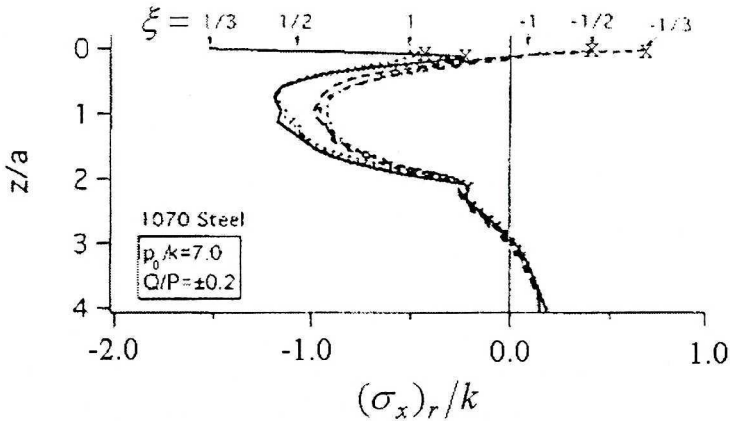

Fig. 5. Residual stress in longitudinal direction after 40 rolling passes (according to Ref. [12])

In our previous work (Ref [13]) it had been shown also that free rolling contact can produce very significant tensile residual stress at the rolled surface. The considered plane problem of an elasto-plastic strip rolled by the elastic cylinder modeled a travel of a train wheel on a rail. The wheel diameter, material properties and loading pressure factor ($p_0/k = 4$) had been chosen to satisfy the rail – wheel rolling conditions. It had been demonstrated also that tangential friction forces between the wheel and the rail due to the brakings and accelerations of the train change dramatically residual stress distributions. They diminish the tension and, in the case of full slip, introduce a significant compression in the surface layer.

However, the influence of many other important factors of the rolling process had not been considered in the mentioned above works. These factors (e.g. loading pressure) can virtually determine the residual stress distributions in the subsurface layer.

The aim of this work is the determination of the influence of some mentioned factors – loading pressure, number of passages, type of state (plane stress versus plane strain), tangential forces – on the residual stress distribution due to the elasto-plastic rolling contact. The numerical analysis conducted using FEM method has been broadly verified by experimental investigations. Experiments have been applied also as the main tool to find

solution in such cases, where using numerical methods is still very expensive (if even possible). The determination of residual stress distribution due to a great number of roller passages (several thousands) is here a good example.

2. Method and range of investigations

Numerical investigations have been conducted by the FEM method using the SEGLA program developed by the authors, as well as the professional ANSYS program. The SEGLA program described in Ref. [13] has been adjusted: large strains and stress effect on the stiffness matrix have been introduced. Such adjustment secured the correct numerical analysis of the rolling process in the plane stress, as well as for high loading factors in the plane strain, where large strains have been playing a major role.

The loading factor p_0/k where $k = R_e/\sqrt{3}$; R_e – yield point) has been evaluated with respect to the maximum Hertz pressure value p_0 computed for the given normal loading force P. The normal pressure distribution between the roller and the strip is, of course, different than the Hertz one and depends on several factors: plastic strains, values and directions of tangential forces due to braking and accelerations, etc. However, to establish the normalized, comparable measure of the loading factor, the p_0 value has been used for all further considerations. It is worth to mention that the maximum values of the real normal pressure are close to p_0 (the differences are a few percent excluding the case of full slip – Fig. 17a, ref. [13]).

The problem of the plane elasto-plastic strip rolled by an elastic cylinder has been computed using the mesh of elements (similar for both programs) shown in Fig. 6. It consists of 6700 elements, 111 nodes that can enter the contact and 20 contact elements (all together 6900 d.f.). The element dimensions are considerably smaller, and the number of elements increases in the contact area, as well as the area of expected major deformations. The dimension of the smallest element is equal approximately $1 \cdot 10^{-4}$ of the cylinder radius R. The rolling bas been carried out along the distance equal ~ 0.2R divided into 2000 substeps; in the unloading (lifting of the cylinder at the end of its travel) 40 substeps have been engaged. The material nonlinearity, as well as the geometrical nonlinearity (changes in geometry, large strains, stress influence on the stiffness matrix, secondary yielding during unloading) have been taken into account during the computation process.
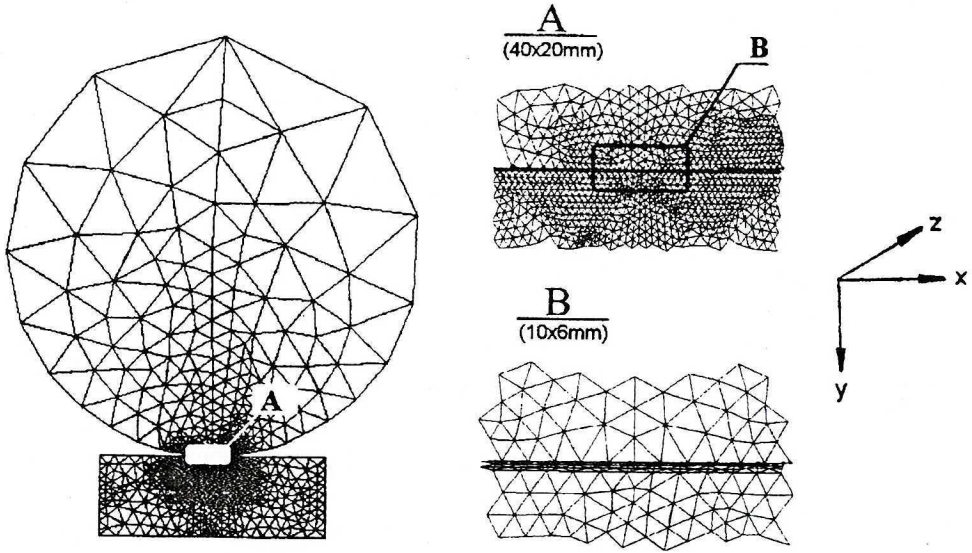
Fig. 6. Elasto-plastic rolling with friction: mesh of elements used in FEM analysis

The bilinear model of the material (Fig. 7b) and the flow rule associated with Huber-Mises-Hencke yield criterion have been applied in calculations. For kinematic linear hardening we have then

$$\sigma_e = \left[\frac{3}{2} (\{s\} - \{\alpha\})(\{s\} - \{\alpha\}) \right]^{\frac{1}{2}},$$

$$F = \sigma_e - R_e = 0,$$

$$\frac{\partial F}{\partial \sigma} = \frac{3}{2\sigma_e} (\{s\} - \{\alpha\}),$$

where

σ_e – the equivalent stress,
R_e – material yield point (in uniaxial state of stress),
$\{s\}$ – deviatoric stress vector,
$\{\alpha\} = \int C \{d\varepsilon_{pl}\}$ – yield surface translation,
$\{\varepsilon_{pl}\}$ – plastic strains,
$C = \dfrac{2EE_u}{3(E - E_u)}$ – material parameter,

E – Young modulus,
E_u – linear strain hardening modulus.
The equivalent stress parameter is

$$\sigma_{epl} = R_e + \frac{EE_u}{E - E_u} \varepsilon_{ple}.$$

The strain hardening modulus E_u had been evaluated from material tension test curve (Fig. 7a), as a slope of the straight line connecting the yield point with the point corresponding to the $\varepsilon = 2.5\%$, The $\sigma - \varepsilon$ relation is almost linear there, and plastic strains usually do not exceed 2,5% during the rolling process; $E_u = 0.024E$. It has been assumed then that the strain hardening modulus (for kinematic hardening) is equal to that in the pure tension.

Similarly, the isotropic linear hardening model has been developed using the same material constants E, E_u and R_e.

It is necessary to emphasize that investigation of an influence of the applied strain hardening model (kinematic, isotropic, mixed) on the residual stress distribution has not been the aim of this work. The model of the material was assumed relatively simple, but enough correct (in the range of the investigations) to verify experimentally numerical findings. It had been checked that, for maximum values of the applied loadings, the kinematics versus isotropic strain hardening models do not provide greater than a few percent differences in residual stress distributions.

A special set-up has been constructed for the experimental investigations. The rolling process has been produced by the slow, quasistatic travel of the strip of the rolled material (the rate of the travel is equal 1 mm/sec), driven using an electric motor and a mechanical device, which creates a reciprocating motion. The multiply passages of the roller (which only rotates without travel) in two directions – forth and back – have been carried out automatically, one way motion was controlled manually. The roller (wheel) hardness number is much greater (~50 HRC) than that of the material of the strip, which secures that the roller remains always in the elastic state. Tangential forces in the contact area are introduced by braking the wheel by the special device. The braking force could be changed from zero to such a value, which corresponds to the full slip (the wheel does not rotate). The running surface has been covered by different powders creating required friction coefficients. The friction forces have been determined experimentally. The setup makes it possible to conduct the experiments with normal loading forces equal $10 \div 100$ KN and braking frictional forces $0 \div 20$ KN. The loading forces are applied by a set of heavy-duty springs.

The setup allows us to produce a multiple reciprocating rolling as well as an multiple one way rolling. Both types of motion often occur in engineering practice. The one way motion deepens permanent tangential deformation in the surface layer. Residual stress distributions, however, are independent of the direction of rolling.

The plane state of stress has been created assuming that the small thickness of the strip equal 10 mm (compared to the wheel radius $R = 200$ mm) secures such a state with a good level of accuracy. It should be mentioned here, however, that the ratio of the strip thickness versus the width of the contact area is a little above 1. The condition of plane stress is not fully satisfied then in the narrow roller-strip contact zone. It had been checked numerically several times by the authors (comparing the longitudinal residual stress distributions in z direction obtained from 3-D solution with these for pure plane stress) that it does not introduce the error greater than 8%. In the plane stress case mentioned above, distributions are of course uniform through the thickness of the strip; in the experimental analysis, the average values of residual stress through the thickness have been evaluated.

The plane state of strain bas been modeled compressing the strip by a couple of very stiff jaws, machined from hard steel, and shaped in a special way. The jaws tie up the transversal deformations of the strip; their shape and compressing forces have been calculated numerically, exclusively for each normal loading.

The residual stress distributions created in the strip by the elasto-plastic rolling contact have been evaluated experimentally using a destructive method of dividing the object into elements, combined with the layers removal method. The method has been developed by the authors and is widely described in Ref. [14].
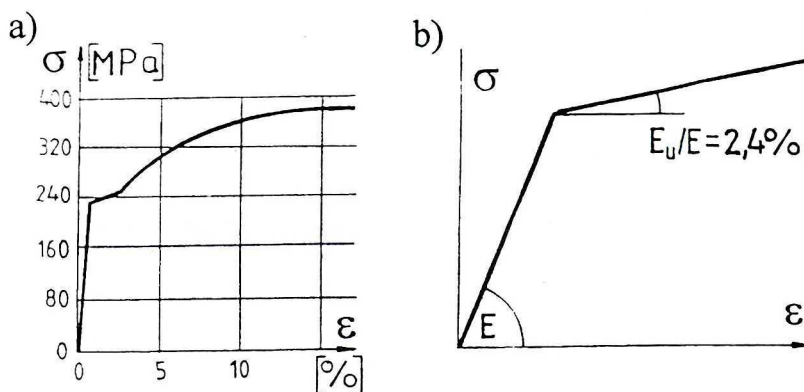

Fig. 7. Material used in investigation; a) real $\sigma - \varepsilon$ relation, b) model applied in numerical calculations

The rolled strip was machined from mild steel, for which the $\sigma - \varepsilon$ relation is shown in Fig. 7a. The same relation applied in numerical calculations demonstrates Fig. 7b.

The range of investigations is presented in Table 1. The friction has been taken into account in all the analyzed cases (the friction coefficients $\mu = 0.1; 0.3$). The free rolling means that the slip at the interface is resisted by friction, but the resultant tangential force T is equal to zero. The tangential force has been determined as

$$T = q\mu P,$$

where P is the normal loading force and q – the coefficient, which determines the applied frictional force. For the free rolling contact of course $q = 0$, in the full slip $q = 1$ for brakings, $q = -1$ for accelerations.

Table 1.

		Numerical investigations	Experimental investigations
1.	State	• Plane stress • Plane strain	• Plane stress • Plane strain
2.	Type of loading	• Normal • Normal with braking $\mu = 0.3$; $q = 0.3$; 0.75; 1.0;	• Normal • Normal + braking $\mu = 0.3$; $q = 0.75$;
3.	Load factor $\dfrac{p_0}{k}$ $k = R_e / \sqrt{3}$ R_e – yield point of the material p_0 = maximum Hertz normal pressure	$p_0/k = 3.0 \div 8.5$	$p_0/k = 4.0$; 5.15; 6.0
4.	Number of passages	1	$1 \div 7000$
5.	Investigated material: elastic properties	• $R_e = 502$ MPa; $k = 290$ MPa • $R_e = 240$ MPa; $k = 140$ MPa	• $R_e = 240$ MPa; $k = 140$ MPa
6.	Investigated material: model of hardening	• kinematic linear hardening	• real, approx. linear
7.	Rolling geometry	Roller (wheel) radius R • $R = 457$ mm • $R = 200$ mm one half of the width of the Hertzian contact area • $a = 9.65$ mm • $a = 1.5 \div 4.3$ mm	• $R = 200$ mm • $a = 2 \div 3$ mm

3. Results of investigations and their analysis

The distributions of the longitudinal σ_x^r residual stress component for the plane state of stress are shown in Fig. 8. The results of numerical investigations are compared with experiments. Both, for the free rolling and the rolling with braking the loading pressures $p_0/k = 4.0$ have been applied.

The residual stress distributions, obtained numerically and experimentally, being in very good agreement qualitatively, differ quantitatively, especially in maximum stress values in the thin subsurface layer. It is due to the simplifying assumptions in numerical and experimental investigations, as well as due to imperfections in the numerical procedure. The sources of major errors are:
- The simplifying assumptions in the model of material.
- The inaccuracy of the residual stress measurements – especially the nonuniformity of the thickness of the removed thin layers (~0.05 mm) in the subsurface area, averaging the measurements through the thickness of the strip, neglecting other than longitudinal stress components, etc.
- The convergence and inaccuracy of numerical calculations.

It is necessary to emphasize that, generally, quite significant differences between measured and computed values of residual stress occur in investigatory practice. The good example provide the curves shown in Fig. 4 (Ref. [4]). The differences between computed and obtained experimentally residual stress values are much greater there than 50%.

The distributions for the free rolling are shown in Fig. 8a (solid line – results obtained numerically, dash line – experimentally). On the rolled surface, σ_x^r reaches the very high positive value ($\sigma_x^r/k =\sim 1.6$ obtained numerically, $\sigma_x^r/k = 1.29$ – experimentally, then rapidly dropping changes the sign and at the depth equal about 2 mm ($y/a =\sim 1$, where $a =\sim 2.0$ mm) reaches maximum negative value of $\sigma_x^r/k = -0.4$ (-0.48 experimentally). For $y/a \cong 4$, the stress stabilizes at about zero value. In the plane stress, σ_z^r is equal zero, and σ_y^r residual stress component reaches relatively small values. It is necessary to emphasize that the high tensile stress on the surface is the result of a large plastic elongation in the transversal (z) direction produced by the rolling on the surface and in the surface vicinity (there is a freedom of deformations in this direction in the plane stress). The following contraction phenomenon (shortening in the longitudinal direction), described by the Poisson's ratio, produces significant tension (tensile longitudinal residual stress) in this direction as a final effect.

The results of numerical analysis for the same loading pressure, but with additional tangential forces due to braking: $T_1 = 0.75\mu P$ and $T_2 = 1.0\mu P$ are shown in Figures 8b (solid line) and 8c, respectively. Fig. 8b presents the corresponding experimental curve for $T_1 = 0.75\mu P$ case (dash line). The slip

introduces the qualitative change: the σ_x^r stress component at the surface dramatically drops down reaching the negative value for the full slip $T_2 = 1.0\mu P$. Again, the experiments generally confirm here the numerical findings. The reason of the described change is that shear tractions introduce an elongation in the longitudinal direction (x) in the surface layer, diminishing the mentioned previously shortening effect due to the rolling. As a result, tensile residual stress on the surface decreases and even changes into compressive.
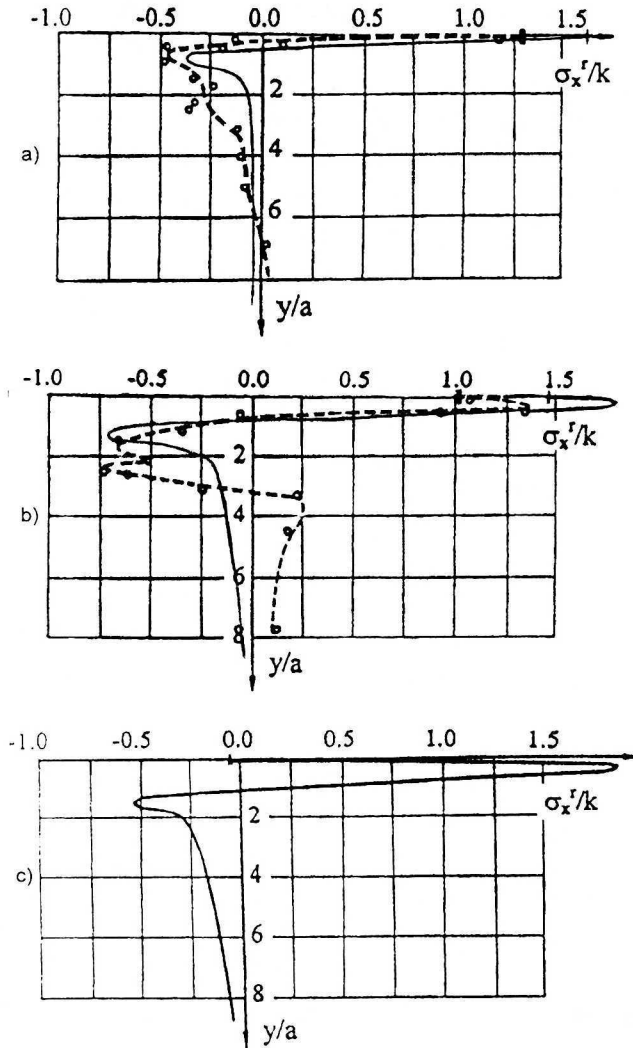

Fig. 8. Distributions of longitudinal residual stress component (σ_x^r) in plane stress for free rolling and rolling with braking: material $R_r = 240$ MPa, roller radius $R = 200$ mm; a) $p_0/k = 4.0$, free rolling, b) $p_0/k = 4.0$, rolling with braking $q = 0.75$, $\mu = 0.3$, c) $p_0/k = 4.0$, rolling with braking $q = 1.0$, $\mu = 0.3$, —— numerical solution; ----- experiments
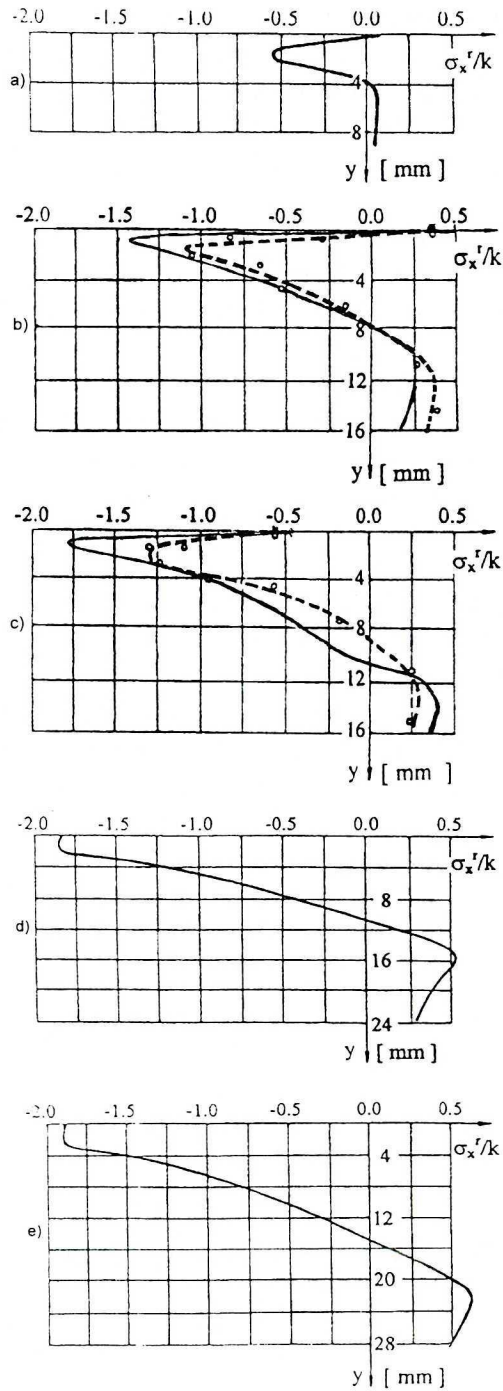
Fig. 9. Distributions of longitudinal residual stress component (σ_x^r) in plane strain for free rolling: material $R_c = 240$ MPa, roller radius $R = 200$ mm; a) $p_0/k = 4,0$; b) $p_0/k = 5.15$; c) $p_0/k = 6.0$; d) $p_0/k = 7.3$; e) $p_0/k = 8.5$; —— numerical solution; ----- experiments

The influence of the normal loading (described by the ratio p_0/k) on the σ_x^r residual stress component distribution in plane strain, for the free rolling situation, is presented in Figures 9a,b,c,d,e by the solid lines (results of numerical analysis) and Figures 9b,c by the dash lines (experimental findings). The distributions are shown for $p_0/k = 4.0;5.15;6.0;7.3;8.5$, respectively.

The difference between plane stress and plane strain is obvious. Generally, in plane stress, very high tension appears on the surface, with small compression at same depth beneath. In plane strain, the situation for average values p_0/k (e.g. $p_0/k = 4.5;5.15;$) is almost opposite: the relatively smaller positive residual stresses are created on the surface and high compression beneath. Growth of the p_0/k changes the distribution dramatically: the tension on the surface diminishes, then σ_x^r becomes there negative, its absolute value quickly increases and, at the end, stabilizes at the high level of compression. The range of the compressive residual stress area (measured as a depth from the surface) also significantly increases as a function of p_0/k: for the high p_0/k values (e.g. $p_0/k = 7.3;8.5$) the surface layer of the considerable thickness develops where σ_x^r keeps almost constant high compressive value. The thickness of this layer increases with the p_0/k ratio growth.

The residual stress distribution obtained experimentally for $p_0/k = 5.15;6.0$ (dash lines in Figures 9b,c) confirm the numerical findings with the fair level of accuracy. Serious technical difficulties have made experimental tests for higher p_0/k values impossible.
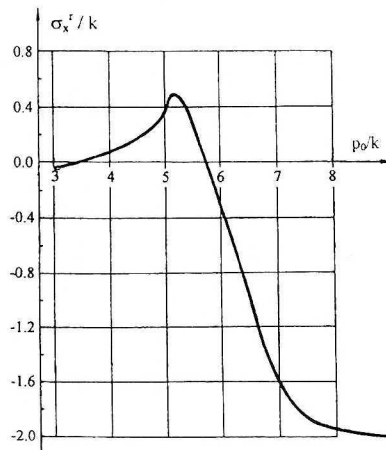

Fig. 10. Longitudinal residual stress component (σ_x^r) at the surface as a function of p_0/k ratio: plane strain, free rolling, material $R_e = 240$ MPa, roller radius $R = 200$ mm

The value of the σ_x^r residual stress component on the rolled surface as a function of the loading pressure factor p_0/k is shown in Fig. 10. The curve

bas been constructed using data obtained by the numerical calculations – the stress distributions presented in Fig. 9 and other similar, not shown in this paper. The longitudinal residual stress on the surface (σ_x^r), that equals about zero for small p_0/k ratio, reaches maximum positive ($\sigma_x^r/k \cong 0.6$) for $p_0/k \cong 5.15$ and then rapidly drops stabilizing on high compression.

It is necessary to emphasize that figures presented here have been found for some determined material of the rolled strip (mild steel, $R_e = 240$ MPa). The numerical investigations of other materials – hard steels (in small part presented in our former work Ref. [13]) – demonstrate very similar qualitative behavior of the residual stress, but quantitative data, especially the level and the peak position of the positive p_0/k, can be different. Generally, in the plane strain case, where transversal deformations are tied up, the first and maximum plastic flow occurs in x direction at same depth beneath the surface in the vicinity of Belaev points. That answers the question, why on the surface, for small and average p_0/k, the positive σ_x^r is present. For the high loading pressure, although maximum yielding remains at the same depth, plastic strains on the surface increase dramatically, becoming not much smaller than these in the vicinity of Belaev points (for small and average p_0/k values plastic strains at the surface are equal almost zero). As the result, high compression starts on the surface and remains (for $p_0/k > 7.3$) almost the same in subsurface area up to same depth. To illustrate the above explanation, the equivalent residual plastic strain distributions for $p_0/k = 5.15$ and $p_0/k = 7.3$ are exemplified in Fig. 11.
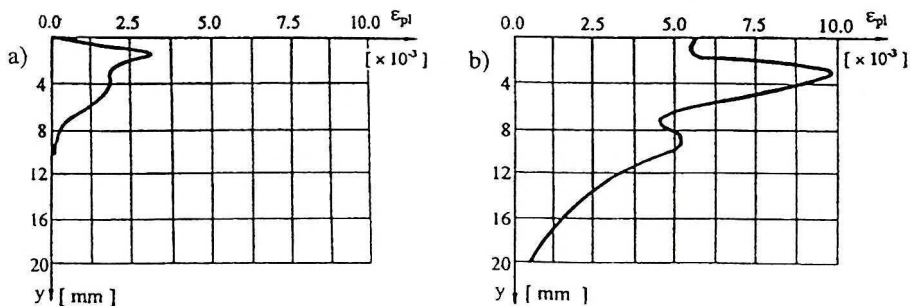

Fig. 11. Equivalent residual plastic strain distributions for free rolling in plane strain: material $R_e = 240$ MPa, roller radius $R = 200$ mm; a) $p_0/k = 5.15$; b) $p_0/k = 7.3$

The influence of tangential forces (for rolling with braking) on the residual stress distribution in plane strain is shown in Fig. 12. In Figures 12a and 12b, the longitudinal (σ_x^r) and transversal (σ_z^r) stress components for average value $p_0/k = 5.15$ are presented, respectively. Figs. 12c and 12d show the same components for high loading pressure $p_0/k = 7.3$. It is necessary to

remind that for $p_0/k = 5.15$, σ_x^r residual stress reaches its maximum possible value (tensile) on the rolled surface (Fig. 10).

The final impact of frictional forces in the contact area on the residual stress distribution is similar to that in the plane stress case, although reasons are different. It is well known that the shear traction at the interface influences the point of maximum yield: in plane strain, with increasing friction, it approaches the surface, but the local peak remains also in the vicinity of Belaev points. As a results, the absolute value of longitudinal residual stress σ_x^r reaches several peaks and – if tensile on the surface – drops there dramatically adopting, for a significant value of tangential force, the negative sign. These effects are clearly demonstrated in Fig. 12a for $p_0/k = 5.15$, if compared with the distribution for the same p_0/k ratio but for free rolling (Fig. 9b).
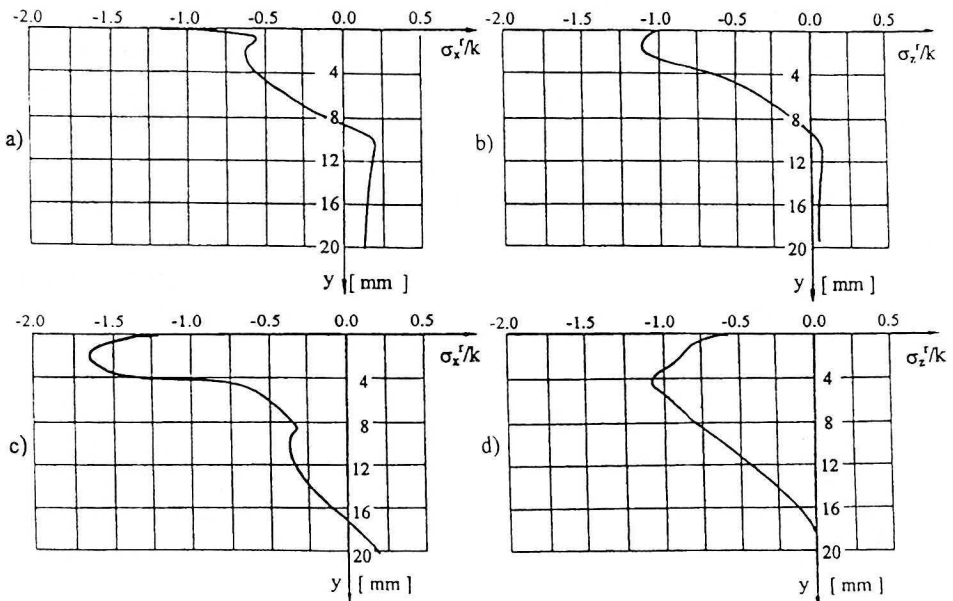

Fig. 12. Distributions of longitudinal (σ_x^r) and transversal (σ_z^r) residual stress components in plane strain for rolling with braking: $q = 1.0$, $\mu = 0.3$, material $R_r = 240$ MPa, roller radius $R = 200$ mm; a) σ_x^r; $p_0/k = 5.15$; b) σ_z^r; $p_0/k = 5.15$; c) σ_x^r; $p_0/k = 7.3$; d) σ_z^r; $p_0/k = 7.3$;

The situation changes for high loading pressure factor ($p_0/k = 7.3$ – Figures 12c,d). σ_x^r reaches in the free rolling its maximum possible negative value in the surface layer (Fig. 9d) higher than the yield point of the material and almost equal to the equivalent stress corresponding to the equivalent strain[1]). Applying then an additional friction force in the contact area, one

---

[1] Because the linear strain hardening bas been applied in computations and because at the considered depth, σ_y^r is very small and negative $|\sigma_z^r| < |\sigma_x^r|$.

cannot increase the compression at the surface but, if any change of residual stress distribution is possible, can only decrease there the absolute value of the stress. This last effect is indicated in Figs. 12c and 12d, where the bends of the curves near the rolled surface produce the significant decrement of the both, longitudinal and transversal components of the residual stress.

The last problem investigated in this work is the influence of the number of passages of the roller (wheel) on the residual stress distribution, if the applied loading pressure slightly exceeds the shakedown limit p_o^s. The problem is of a great interest in such cases, where dynamic and other additional effects cause that the loading pressure appears to be greater than that assumed theoretically. The process of residual stress creation in rails represents here a very important example; therefore the multiply recip-rocating rolling had been investigated.

The shakedown limit for plane strain in terms of the maximum loading pressure equals $p_o^s = 4k$. In Fig 13, the longitudinal (σ_x^r) residual stress distributions are shown for $p_0/k = 5.15$, in plane strain. For this p_0/k ratio, σ_x^r reaches its maximum positive (tensile) value on the rolled surface. All the presented curves are the result of experimental findings; using the numerical calculations for modeling thousands of passages is still to expensive if even possible.

Fig 13a shows the (σ_x^r) stress component distribution created by the one passage obtained many times experimentally. The maximum tension $\sigma_x^r/k = 0.6 \div 0.7$ appears on the surface, maximum compression at the depth equal ~2mm. The compressive stress area reaches ~ 10mm beneath the surface.

The distribution after 5 passages remains almost the same (Fig 13b): small odifferences are more the effect of the measurement error than of the change of the loading conditions.

The results of 21 passages obviously differ from the two former distributions. Although the value of maximum compression as well as the range of the compressive stress changes unsignificantly, the surface residual stress indicates very significant decrement and drops below its positive value. Moreover, in the very close vicinity of the surface, the curve bends rapidly and σ_x^r increases from the high compression on the surface to much smaller but also compressive value at the small depth beneath the surface.

The described-above effects increase to 50 passages, and then remain practically constant, independently of the number of passages (the highest final number is 6918). Fig 14 presents the picture of the variation of the surface longitudinal residual stress component as a function of $\ln N$ (where N is the number of passages). The relation is similar to the Wöhler diagram for

fatigue test. The curve consist of two straight lines, of which the first one, inclined with respect to the ln$N$ axis, describes the residual stress change, and the second one – parallel – represents the compressive stress level, bellow which the longitudinal residual stress component on the surface never drops, independently of the number of passages.
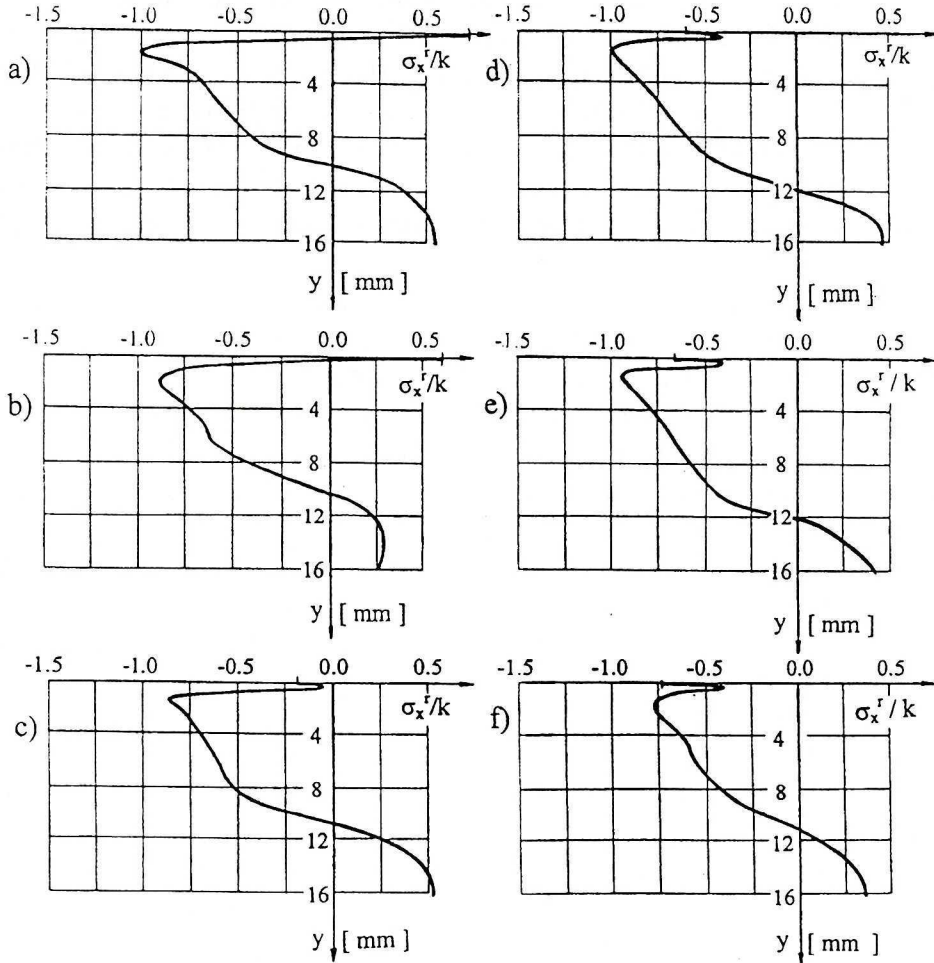

Fig. 13. Distributions of longitudinal residual stress component (σ_x^r) in plane strain for free rolling – experiments: material R_e = 240 MPa; roller radius R = 200 mm, p_0/k = 5.15; a) one passage; b) 5 passages; c) 21 passages; d) 50 passages; e) 100 passages; f) 6918 passages

It would be interesting to compare the presented-above findings with these for one – way multiply rolling. The authors are planning such investigations in near future. However, it has been shown, in Ref. [12], that the number of rolling passes to stabilize the residual stress distribution is similar and equal to ~40.
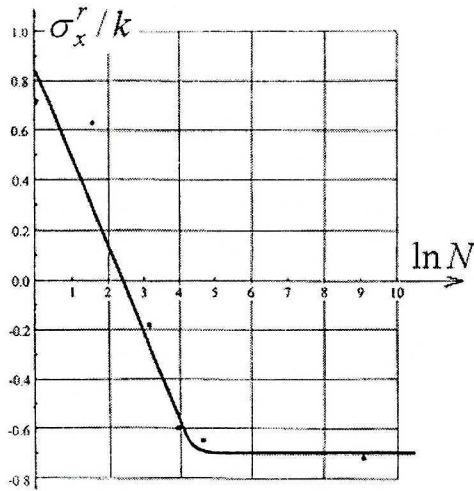
Fig. 14. Longitudinal residual stress component at the rolled surface as a function of the number of passages: material $R_e = 240$ MPa, roller radius $R = 200$ mm, $p_0/k = 5.15$

4. Discussion and conclusions

The presented effects of elasto-plastic rolling in different conditions allow us to determine the impact of the most important factors on residual stress distributions generally, and in the subsurface layer particularly. Experimental findings have confirmed the results of numerical analysis and have delivered also many important bits of information not possible to obtain by computation. The final main conclusions are as follows:

1. Residual longitudinal stresses always reach high tensile value on the rolled surface for free rolling in plane stress. It is a result of the large plastic elongation in the transversal (z) direction produced by the rolling in the vicinity of the surface, and the following contraction (shortening) in the longitudinal (x) direction. The freedom of deformations in z direction ($\sigma_z^r = 0$) creates such effects.

2. Additional tangential forces in the contact area due to the braking and acceleration cause the qualitative change in the stress distribution in plane stress. Shear tractions introduce elongation in the longitudinal direction (x) into the surface layer, diminishing the mentioned-above shortening. As a result, tensile residual stress on the surface decreases dramatically (the distribution curve rapidly bends close to the surface) and for full slip it reaches even negative value (compression).

3. The distribution of residual stress in plane strain is in same sense opposite to that in plane stress. In plane stress, appears very high tension on the

surface and small compression beneath. In plane strain, for average values of the loading pressure factor p_0/k, relatively smaller positive residual stresses are created on the surface and high compression beneath.

4. The most important factor, which influences very strongly residual stress distribution, is the normal loading pressure described by the p_0/k ratio. The increase of p_0/k causes the rapid drop of (σ_x^r) and (σ_z^r) residual stress components on the surface that, for $p_0/k > 7.3$, stabilize on high compression, being almost uniform in the surface layer of the finite thickness up to same depth. The surface stress component (σ_x^r) indicates the maximum tensile value (quite considerable) for some average p_0/k ratio. These effects in plane strain are the results of the existence of Belaev points at same depth bellow the surface, where the first and maximum plastic flows occur if transversal deformations are tied up. Considerable plastic deformation in the vicinity of Belaev points, followed by small deformation on the surface for the average p_0/k, creates there the tension. With the p_0/k growth, the plastic deformation on the surface increases to the level almost equal to that in Belaev points and high compression appears in the surface layer.

5. The influence of frictional forces in the contact area in plane strain is similar to that in plane stress, although the reasons are different. In plane strain, shear traction at the interface shifts the point of maximum yield: with increasing friction it approaches the surface. Tensile residual stress diminishes rapidly assuming significant values of negative sign. However, the application of an additional friction force in the situation of heavy rolling (high p_0/k ratio), when in the surface layer the residual stress already has reached its maximum possible negative value, leads to diminishing of the compression on the surface.

6. The number of passages N has a significant impact on the residual stress distribution, if the applied loading pressure exceeds the shakedown limit. The general distribution and the value of the longitudinal residual stress on the surface are independent of N up to a few passages $(5 \div 7)$, then σ_x^r constantly drops and, at the end, it stabilizes at a constant level of considerable compression for $N = 50 \div 100$ passages.

All the above conclusions are based not only on the investigations conducted for mild steel ($R_e = 240$ MPa). Such steel had been chosen to make possible the experimental tests in plane strain for high p_0/k value. Using harder materials, followed by applying much higher normal loading, was not possible in laboratory conditions. Verifying experimentally numerical

calculations, as well as conducting measurements for a great number of passages, seemed to be enough important to accept such a choice of the investigated material.

The numerical calculations, however, have been performed also for another material (hard steel, $R_e = 502$ MPa) providing a general confirmation of the presented findings. The figures brought in this paper could be different for different materials, but the qualitative behavior of residual stress remains the same.

REFERENCES

[1] Yu M. M., Morgan B., Keer L. M.: A direct analysis of three-dimensional elastic-plastic rolling contact. ASME J. Tribology 117 (1995).

[2] Kulkarni S. M., Hahn G.T., Rubin C. A., Bhargava V.: Elasto-plastic finite element analysis of three-dimensional pure rolling contact at the shakedown limit. ASME J. Appl. Mech. 57, 57÷65 (1990).

[3] Yu C. C., Morgan B., Keer L. M.: A simplified direct method for cycling strain calculations: repeated rolling/sliding contact on a case-hardened half-plane. ASME J. Tribology 118 (1996).

[4] Howell M., Hahn G. T., Rubin C. A., Mc Dowell D. L.: Finite element analysis of rolling contact for nonlinear kinematic hardening bearing steel. ASME J. Tribology, 117 (1995).

[5] Jiang Y., Sehitoglu H.: Rolling contact stress analysis with the application of a new plasticity model. Elsevier. Wear 191 (1996), pp. 35÷44.

[6] Jiang Y., Sehitoglu H.: Modeling of cyclic ratchetting plasticity. Part I: Development of constitutive relations. Journal of Applied Mechanics. Vol. 63, 1996, pp. 720÷725.

[7] Jiang Y., Sehitoglu H.: Modeling of cyclic ratchetting plasticity. Part II: Comparison of model simulations with experiments. Journal of Applied Mechanics. Vol. 63, 1996, pp. 726÷733.

[8] Yu C. C., Keer L. M., Steele R. K.: Three-dimensional residual stress effects on the fatigue crack initiation in rails. ASME Journal of Tribology. Vol. 119, 1997, pp. 660÷666.

[9] Jiang Y., Sehitoglu H.: A model for rolling contact failure. Wear 224 (1999), pp. 38÷49.

[10] Ringsberg J. W., Loo-Morrey M., Josefson B. L., Kapoor A., Beynon J. H.: Prediction of fatigue crack initiation for rolling contact fatigue. International Journal of Fatigue, 22 (2000) pp. 205÷215.

[11] Jiang Y., Chang J., Xu B.: Elastic-plastic Finite Element Stress analysis of Two-Dimensional Rolling Contact. ASTM STP 1339. 2001, pp. 37÷54.

[12] Xu B., Jiang Y.: Elastic-plasstic finite element analysis of partial slip rolling contact. ASME J. of Tribology, 124 (2002), pp. 20÷26.

[13] Bijak-Żochowski M., Marek P., Residual stress in some elasto-plastic problems of rolling contact with friction. Int. J. Mech. Sci., Vol. 39, No 1 (1997).

[14] Bijak-Żochowski M., Tracz M.: Investigation of residual stress distribution in a rail head. Journal of Strain Analysis. Vol. 28, No 1 (1994).

O naprężeniach własnych wywołanych sprężysto-plastycznym kontaktem przy rolowaniu

Streszczenie

Sposób tworzenia i ostateczny rozkład naprężeń własnych wywołanych w procesie rolowania są ważne i z poznawczego i praktycznego punktu widzenia. Naprężenia własne mogą być wprowadzone zarówno przez kontrolowane procesy technologiczne w celu zwiększenia wytrzymałości (np. rolowanie na zimno czopów, gwintów itp.), jak i niezamierzony efekt eksploatacji obiektu. Naprężenia własne w szynach kolejowych powstają właśnie w ten drugi sposób: wpływają one silnie na procesy pękania i trwałość szyny.

Rozkłady naprężeń własnych wprowadzonych sprężysto-plastycznym rolowaniem zależą od wielu czynników: wielkości maksymalnych nacisków w kontakcie tocznym, charakteru ruchu (rolowanie czyste, z siłami stycznymi wywołanymi hamowaniem i przyspieszaniem) liczby przejazdów etc. Badania prowadzone tu przez bardzo wielu autorów nie dostarczyły wszakże jednoznacznego rozwiązania nawet dla czystego rolowania. Szczególnie nie jest jasne jakie naprężenia powstają w cienkiej warstwie podpowierzchniowej oraz, czy i kiedy mogą być rozciągające na samej powierzchni.

Celem tej pracy jest określenie wpływu niektórych ze wspomnianych czynników na rozkłady naprężeń własnych. Analizę przeprowadzono numerycznie stosując Metodę Elementów Skończonych. Wyniki szeroko zweryfikowano doświadczalnie.